

Facile method to prepare copper-doped LiNbO₃ nanocrystals

Xiaobin Liu, Wenxiu Que, Yonglei Xing, Zuoli He, Yucheng He

Electronic Materials Research Laboratory, International Center for Dielectric Research, Xi'an Jiaotong University, Xi'an 710049, Shaanxi, People's Republic of China
E-mail: wxque@mail.xjtu.edu.cn

Published in Micro & Nano Letters; Received on 2nd March 2015; Revised on 11th April 2015; Accepted on 13th April 2015

A facile method to prepare copper-doped LiNbO₃ nanocrystalline is reported. It should be mentioned here that the harmless citric acid plays a key role in soluble niobate at first and in the formation of the uniform gel. A detail thermal behaviour of the as-obtained gel was investigated by thermogravimetry and differential thermal analysis. The crystal structure, elemental composition and microstructural properties were characterised by X-ray diffraction analysis, X-ray photoelectron spectroscopy and scanning electron microscopy. Results indicate that a pure phase similar to LiNbO₃, which has the cell parameters of $a = b = 5.150(5)$ Å and $c = 13.896(9)$ Å, can be obtained at a low temperature (~550°C) and the mean particle size of the as-synthesised nanocrystalline is about 40 nm.

1. Introduction: Over the last decade, nanomaterials have been the subject of enormous interest because of their extremely small feature size and potential for wide-ranging industrial, biomedical and electronic applications [1]. In many nanoscale materials, an important aspect is the vastly increased ratio of surface area to volume, which causes the 'quantum size effect' where the optical and electronic properties of solids are altered with changing particle size [2–4].

Lithium niobate (LiNbO₃) has been extensively researched for its excellent ferroelectric, piezoelectric, dielectric, pyroelectric, electrooptical and non-linear optical properties [5–7]. Due to its excellent properties, it has been intensely studied for applications in holographic memories, second harmonic generation and electro-optics. However, for the performance modification of materials including LiNbO₃, doping is a commonly used and efficient method [8–10]. In this Letter, we report a facile method to prepare the copper (Cu)-doped LiNbO₃ nanocrystals at low temperatures using low-cost raw materials including Li₂CO₃, Nb₂O₅ and Cu(NO₃)₂·3H₂O, where the nanocrystals have gained potential applications in dielectric (including ferroelectric and piezoelectric) and photoelectric devices as well as a photocatalyst. The detailed thermal behaviour, crystal structure, element composition and microstructural property as well as optical properties were investigated. Furthermore, other metal ions (e.g. Fe, Mn, Ni etc.) should also be introduced by only replacing water-soluble metal salts.

2. Experimental procedure

2.1. Synthesis of niobium citrate solution: The preparation process is shown in Fig. 1, and it should be mentioned that deionised (DI) water was used throughout the preparation. Nb₂O₅ (>99.99) powder and KOH (>99.9%) powder with a mass ratio of 1:10 were placed in a crucible and calcined at 400°C for 2 h. Then, the calcined powder was dissolved in DI water. After centrifugation, the upper transparent solution was retained. Subsequent to that, an appropriate amount of nitric acid was added to the as-obtained clear solution to produce Nb(OH)₅·*n*H₂O precipitate, which was washed several times until the solution was neutral. Then it was continuously stirred at 80°C, until the Nb(OH)₅·*n*H₂O precipitate was dissolved in excess citric acid solution to obtain transparent niobium citrate solution. According to the solution homogeneity, the solution amount of 10 ml was dried and then calcined at 900°C in air, and the calcined powder (Nb₂O₅) mass was weighed to determine the amount of Nb per unit volume of niobium citrate solution.

2.2. Fabrication of lithium Cu-niobate nanocrystals: As shown in Fig. 1 (right), a molar ratio 1:3:1 of Li₂CO₃, Nb source and Cu(NO₃)₂ was used. Lithium carbonate and copper nitrate were added to niobium citrate solution and then ethylene glycol of 10% in volume was also added to the solution. After stirring, the as-obtained blue solution was dried in an oven at 100°C to form a dry gel and thus the dry gel was further calcined. Next, the black calcined powders were washed in dilute nitric acid to remove black copper oxide powders and then were washed using DI water. Finally, the obtained powder was dried at 80°C in air.

2.3. Characterisation: Decomposition and crystallisation behaviour of the polymeric precursors were analysed by thermogravimetry and differential thermal analysis (TG/DTA, STA449C, GER) at a heating rate of 15°C/min. Crystalline properties of the as-prepared samples were characterised by powder X-ray diffractometry analysis (D/max-2200, Rigaku, Japan) using Cu K α radiation. Composition of the products was performed by using X-ray photoelectron spectroscopy (XPS), which was obtained by Axis Ultra, Kratos (UK) using monochromatic Al K α radiation (150 W, 15 kV, 1486.6 eV) under a vacuum pressure of 10^{−9} Torr. All the binding energies were referenced to the C1s peak (284.80 eV) from hydrocarbons adsorbed onto the surface of the samples. Morphological properties of the products were observed by a scanning electron microscope (SEM, Quanta F250), all the images of which were obtained under a high vacuum mode. UV–vis diffuse reflectance spectra of the as-obtained powder were collected using a Jasco V-570 with the help of an integrating sphere. A reference sample was made with barium sulfate powder. The data were plotted according to the function $F(R) = (1 - R_{\infty})^2 / (2R_{\infty})$, where R is the diffuse reflectance based on the Kubelka–Munk theory of diffuse reflectance [11, 12]. The Tauc plot method was used to determine the direct and indirect bandgaps [13].

3. Results and discussion: As shown in Fig. 2, thermodynamic behaviours in the heating process were investigated by the TG–DSC curves obtained at a heating rate of 15°C/min. First, the slight endothermic peak at 100°C, which corresponds to about 8% weight loss, is due to the thermal evaporation of water. The exothermic peaks centred at 292, 334.5 and 457°C are due to the decomposition of glycol, nitrate and citrate, respectively. It should be mentioned here that the exothermic peak at 510°C, which corresponds to the start point of the level TG curve, is due to the crystallisation peak, indicating that the crystal phase can be

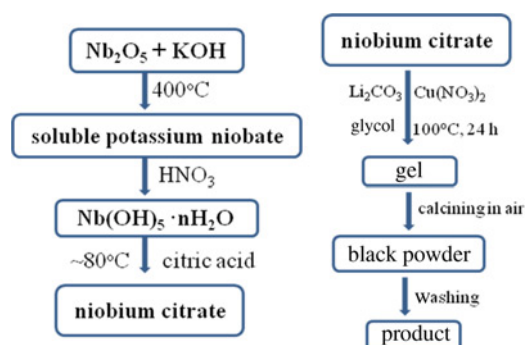


Figure 1 Synthesis process of niobium citrate and Cu-doped LiNbO₃

obtained at a low temperature. Therefore, calcination temperatures of higher than 510°C were selected.

Fig. 3 shows XRD patterns of the as-obtained gel with different calcination temperatures. Moreover, the calculation XRD pattern corresponding to PDF #01-074-2236 was obtained from the LiNbO₃ crystal structure (rhombohedral structure [R3C (161)], data_28294-ICSD), which is shown in the inset of Fig. 3. It can be clearly seen that all the XRD patterns are consistent with the calculation XRD pattern, which shows that the single-phase structure compound can be obtained at the experimental temperature. In addition, the obtained powder has a rhombohedral structure with refinement cell parameters $a = b = 5.150(5)$ Å and $c = 13.896(9)$ Å (calculated from JADE software).

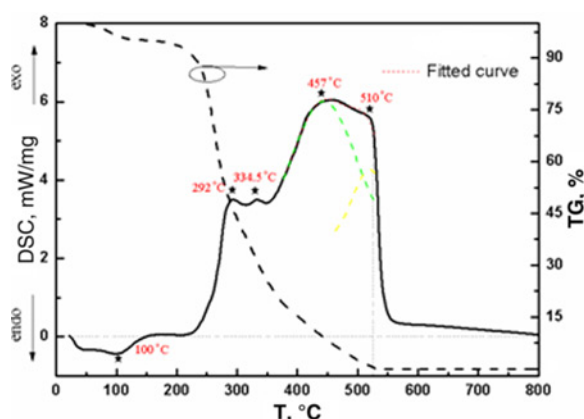


Figure 2 TG-DSC curves of dry gel with heating process

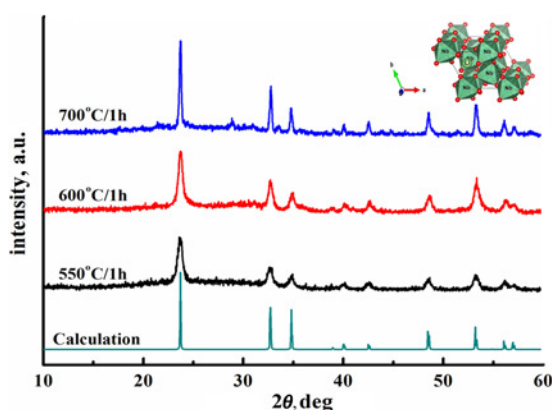


Figure 3 XRD patterns of dry gel in different calcination temperatures
Inset: LiNbO₃ crystal structure (data_28294-ICSD)

Fig. 4 shows the survey XPS spectrum, Cu 2p and Li 1s XPS spectra of the obtained powder. As shown in the full XPS spectrum (Fig. 4a), the obtained powder consists of Li, Cu, Nb and O elements and also illustrates that the Cu atom enters into the LiNbO₃ crystal lattice. The Li 1s peak is relatively low in the survey spectrum, which may be related to the low sensitivity factor of the Li element. Importantly, according to the XPS data of the Cu 2p spectra (Fig. 4b), the main valence of Cu element can be determined to be +2 as the satellite peak appears.

Figs. 5a and b show the Tauc plots of $[F(R)h\nu]^n$ against $[h\nu]$ for the measurement of the direct and indirect bandgap values, $n=2$ and $1/2$, respectively. The results of the obtained bandgap values are shown in Fig. 5. It can be seen that the values decrease from 3.3 to 2.95 eV for direct bandgap and from 3.24 to 2.6 eV for indirect bandgap, which is due to the fact that a new doping level related to Cu element was formed in the forbidden band of LiNbO₃ crystals.

The SEM images of the powder calcined at 550°C are shown in Fig. 6. It can be seen that the particle morphology of the obtained Cu-doped LiNbO₃ is spherical and its mean particle size is about 40 nm, which can be clearly observed in Fig. 6b. In addition, the EDS result of the obtained Cu-doped LiNbO₃ is shown in the inset of Fig. 6a. It must be pointed out that the carbon element is from the black conductive adhesive and the lithium element is not shown because the lithium element cannot be detected by the technology. Importantly, the approximate content of Cu doping was obtained and the value is atomic percentage of ~0.39.

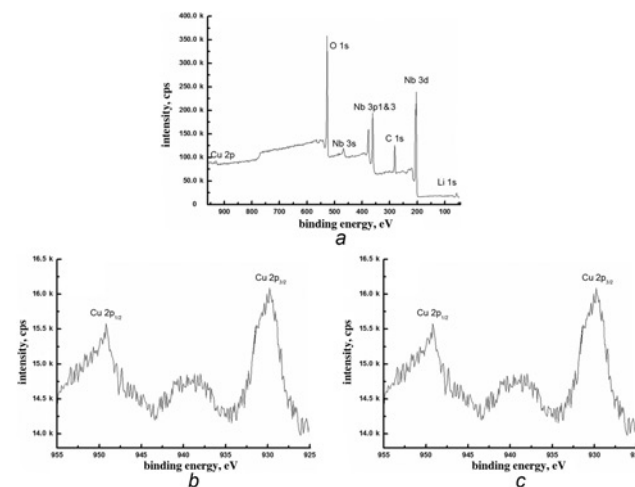


Figure 4 XPS spectra of the sample calcinated at 550°C

a Survey XPS spectrum
b Cu 2p spectrum
c Li 1s XPS spectrum

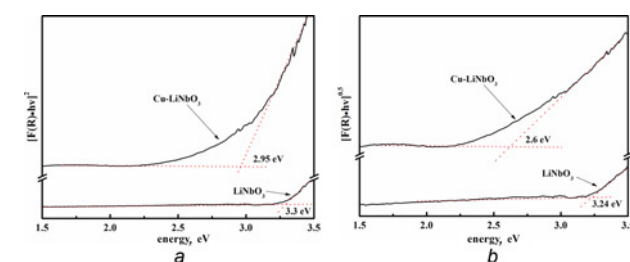


Figure 5 Tauc plots of $[F(R)h\nu]^n$ against $[h\nu]$ for measurement of the direct and indirect bandgap values

a $n=2$
b $n=1/2$

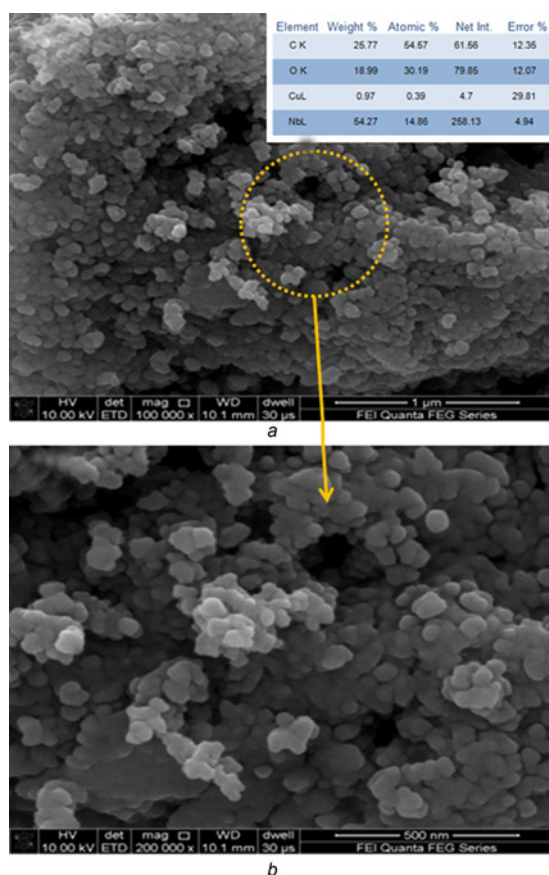


Figure 6 SEM images of the powder calcined at 550°C
 a Low magnification SEM image
 b High magnification SEM image
 Inset: EDX results

4. Conclusion: Cu-doped LiNbO_3 nanocrystalline powder has been successfully synthesised via a facile method. For the full preparation process, harmless citric acid plays an important role. XRD results indicate that a single-phase compound similar to LiNbO_3 can be obtained at a low temperature ($\sim 550^\circ\text{C}$). Its direct and indirect bandgaps were obtained and their values are 2.95 and 2.6 eV, respectively. From the SEM image, the mean particle size of Cu-doped LiNbO_3 is about 40 nm.

5. Acknowledgments: This work was supported by the Research Fund for the Doctoral Program of Higher Education of China under grant 20120201130004, the National Natural Science Foundation of China under grant no. 61078058, the 111 Project of China (B14040) and the Science and Technology Developing Project of Shaanxi Province (2012KW-11). The SEM work was done at the International Centre for Dielectric Research (ICDR), Xi'an Jiaotong University, Xi'an, China; the authors also thank Ms. Dai for her help in using SEM.

6 References

- [1] Hickman K.: 'Nanomaterials: it's a small, small world' (Cambridge Scientific Abstracts, Cambridge, 2002)
- [2] Koch U., Fojtik A., Weller H., *ET AL.*: 'Photochemistry of semiconductor colloids. Preparation of extremely small ZnO particles, fluorescence phenomena and size quantization effects', *Chem. Phys. Lett.*, 1985, **122**, (5), p. 507
- [3] Wang Y., Suna A., Mahler W., *ET AL.*: 'PbS in polymers from molecules to bulk solids', *J. Chem. Phys.*, 1987, **87**, (12), p. 7315
- [4] Choi J., King N., Maggard P.A.: 'Maggard metastable Cu(I) -niobate semiconductor with a low-temperature, nanoparticle-mediated synthesis', *ACS Nano*, 2013, **7**, (2), p. 1699
- [5] Wang K., Li J.F., Liu N.: 'Piezoelectric properties of low-temperature sintered Li modified (Na, K) NbO_3 lead-free ceramics', *Appl. Phys. Lett.*, 2008, **93**, p. 092904
- [6] Chen J., Li Y.D., Lu W.Q., *ET AL.*: 'Observation of surface-plasmon-polariton transmission through a silver film sputtered on a photorefractive substrate', *J. Appl. Phys.*, 2007, **102**, p. 113109
- [7] Sarkisov S.S., Curley M.J., Williams E.K., *ET AL.*: 'Nonlinear optical waveguides produced by MeV ion implantation in LiNbO_3 ', *Nucl. Instrum. Methods Phys. Res. B: Beam Interact. Mater. At.*, 2000, **166**, p. 750
- [8] Kong Y., Liu S., Xu J.: 'Recent advances in the photorefractive of doped lithium niobate crystals (review)', *Materials*, 2012, **5**, p. 1954
- [9] Phillips W., Amodei J.J., Staebler D.L.: 'Optical and holographic storage properties of transition metal doped lithium niobate', *RCA Rev.*, 1972, **33**, p. 94
- [10] McMillen D.K., Hudson T.D., Wagner J., Singleton J.: 'Holographic recording in specially doped lithium niobate crystals', *Opt. Express*, 1998, **2**, p. 491
- [11] Morales A.E., Mora E.S., Pal U.: 'Use of diffuse reflectance spectroscopy for optical characterization of un-supported nanostructures', *Rev. Mex. Fis.*, 2007, **S53**, p. 18
- [12] Kubelka P., Munk F.: 'Ein Beitrag zur Optik der Farbanstriche', *Z. Tech. Phys.*, 1931, **12**, p. 593
- [13] Tauc J., Grigorovici R., Vancu A.: 'Optical properties and electronic structure of amorphous germanium', *Phys. Status Solidi*, 1966, **15**, p. 627